Title
Chemical Genetics of Rapamycin-Insensitive TORC2 in S. cerevisiae

Journal
Cell Reports, 5(6)

ISSN
2639-1856

Authors
Kliegman, Joseph I
Fiedler, Dorothea
Ryan, Colm J
et al.

Publication Date
2013-12-01

DOI
10.1016/j.celrep.2013.11.040

Peer reviewed

Published in final edited form as:
Cell Rep. 2013 December 26; 5(6): 1725–1736. doi:10.1016/j.celrep.2013.11.040.

Chemical-Genetics of Rapamycin-Insensitive TORC2 in *S. cerevisiae*

Joseph I. Kliegman[1,2,3], **Dorothea Fiedler**[4], **Colm J. Ryan**[1,2,5], **Yi-Fan Xu**[4], **Xiao-yang Su**[4], **David Thomas**[4], **Max C. Caccese**[1,2,3], **Ada Cheng**[1,2], **Michael Shales**[1,2], **Joshua D. Rabinowitz**[4], **Nevan J. Krogan**[1,2,6], and **Kevan M. Shokat**[1,2,3]

[1]Department of Cellular and Molecular Pharmacology, University of California, San Francisco, CA, 94158, USA [2]California Institute for Quantitative Biosciences, QB3, San Francisco, CA, 94158, USA [3]Howard Hughes Medical Institute, San Francisco, CA 94158, USA [4]Department of Chemistry, Princeton University, Princeton, NJ 08540, USA [5]School of Computer Science and Informatics, University College Dublin, Dublin 4, Ireland [6]J. David Gladstone Institutes, San Francisco, CA, 94158, USA

Abstract

Current approaches for identifying synergistic targets use cell culture models with combinations of clinically available drugs to see if the combined effect of the combination is better than predicted by their individual efficacy. New techniques are needed to systematically and rationally identify targets and pathways that have a high potential as synergistic targets. In this study, we create a tool to screen and identify molecular targets that may synergize with new inhibitors of TOR (Target of Rapamycin), a conserved protein that is a major integrator of cell proliferation signals in the nutrient-signaling pathway. While clinical results from TORC1 inhibition using rapamycin analogs (that only inhibit TORC1) have been disappointing, trials using inhibitors that also target TORC2 have been promising. To understand the molecular basis for this increased therapeutic efficacy and to discover secondary targets that may have potential in targeted combination therapy, we engineered TOR2 in *S. cerevisiae* to accept an orthogonal inhibitor in order to create the first chemical tool to selectively inhibit TORC2. We used this tool to create a Chemical Epistasis Mini-Array Profile, or ChE-MAP, by measuring interactions between the chemically inhibited TOR2 kinase and a diverse library of deletion mutants. The ChE-MAP identified known TOR components and distinguished between TORC1 (assessed using rapamycin) and TORC2 dependent functions. Results showed a novel TORC2-specific interaction with the pentose phosphate pathway (PPP). We used global metabolic profiling to show that that TORC2 inhibition led to decreases in metabolites specific to the PPP and confirmed that TOR2 was regulating this

To whom correspondence should be addressed: kevan.shokat@ucsf.edu.

Supplemental Data

Supplemental data include 4 figures and 4 tables and can be found at http://cellreports.cell.com/

process using metabolic flux analysis. Regulation of the PPP is a previously unappreciated role for TORC2 that may suggest a role for the complex in balancing the high energy demand required for ribosome biogenesis.

Introduction

Kinase signaling networks are primary regulators of cell growth and division. Improper signaling caused by mutations to kinases is a major driver of cancer progression (Greenman et al., 2007; The Cancer Genome Atlas Research Network et al., 2013; Wood et al., 2007). The success of targeting single kinases has been mixed due to rapidly emerging drug resistance and significant toxicity that limits the use of several of these agents to doses that do not block cancer growth (Boss et al., 2009; Greenman et al., 2007; Haura et al., 2010; The Cancer Genome Atlas Research Network et al., 2013; Wood et al., 2007). In contrast, the vast majority of clinically available therapeutics have multiple targets (Knight et al., 2010; Mestres et al., 2009). Many of these off-targets contribute to the therapeutic efficacy but also increase the toxicity and side effects of these drugs. Many preclinical and clinical studies have empirically searched for synergistic activities of kinase-targeted therapies but systematic studies are far less common. In this study, we endeavor to systematically study synergistic interactions with TOR kinase activity.

TOR is a primary integrator of proliferative signals and aberrant signaling by this kinase contributes to cancer (Casadio et al., 1999; Inoki et al., 2005; Kaeberlein et al., 2005; Martin and Hall, 2005; Tee and Blenis, 2005; Tischmeyer et al., 2003). As clinical use of selective inhibitors of TOR complex 1 (TORC1) (rapamycin and its derivatives, rapalogs) become more widespread in cancer treatment and ATP-competitive inhibitors of both TORC1 and TORC2 (including BEZ235, INK-128/MLN0128, KU-0063794, and WYE-354) reach the clinic, the search for secondary targets to use in combination therapy will gain urgency.

In addition to the clinical utility of an efficient method to find secondary targets to use in combination with TOR inhibitors, we were motivated by the fundamental lack of understanding of TORC2 biology resulting from the lack of pharmacology to selectively inhibit this complex. While prior studies have identified roles for TORC2 in cytoskeletal reorganization, sphingolipid biosynthesis and ribosome biogenesis (Beeler et al., 1998; Breslow et al., 2008; Helliwell et al., 1998b; Roelants et al., 2004; Schmidt et al., 1997; Zinzalla et al., 2011), it has been impossible to monitor these interactions on a rapid timescales possible with drug inhibition. It has also been impossible to specifically trace the function of these interactions to the ‘kinase activity’ of TORC2.

While selective pharmacological inhibition of TORC2 in mammals is not easily achieved since both complexes share the same kinase, *S. cerevisiae* has two distinct kinase genes, TOR1 and TOR2 that can be independently inhibited. TORC1 can contain TOR1 or TOR2 and is rapamycin sensitive. TORC2 only contains TOR2 and is rapamycin insensitive (Loewith et al., 2002). The presence of distinct TOR kinases in yeast is a key advantage that enables independent modification of the active site of TOR2 using chemical genetics to generate a selective inhibitor for a modified allele of TORC2 (Bishop et al., 2000).

To study the selective pharmacology of TORC2 inhibition, we engineered an allele of TOR2 (as-TOR2) to accept an orthogonal kinase inhibitor that would not inhibit TORC1. To generate an unbiased map of the signaling network that TORC2 participates in and to furnish a list of interesting secondary targets for combination therapy, we determined chemical-genetic interactions between the TORC2 kinase and ~1000 non-essential genes in *S. cerevisiae*. For comparison, we generated a chemical genetic interaction dataset using the TORC1 inhibitor rapamycin. This approach enabled independent investigation of genetic interactions arising from the catalytic activity of either TOR complex.

Typically, genetic interactions report on how the function of one gene depends on the function of another. Negative interactions occur when two mutations cause the resulting double mutant to grow worse than expected relative to the growth rate of the two single mutants and indicates the two genes function in redundant or compensatory pathways. Positive interactions occur when the double mutant grows better than expected based on the phenotypes of the two single mutants suggesting the two genes function in the same complex or in a linear pathway (Beltrao et al., 2010; Collins et al., 2007; Fiedler et al., 2009; Kelley and Ideker, 2005; Roguev et al., 2008; Ryan et al., 2012; Schuldiner et al., 2005; Tong et al., 2004). Retaining this framework for interpretation, we developed a new tool for analysis of the dose-dependent effect of selective inhibitors, termed Chemical Epistasis Mini-Array Profile (ChE-MAP).

ChE-MAP is a pharmacological extension of the powerful E-MAP technology that typically relies on the growth phenotype of double deletion mutants (Collins et al., 2010; 2006; Schuldiner et al., 2006) and enables dose-dependent kinase-gene interactions to be identified. The gene interactions are akin to an allelic series from hypomorphic (low dose drug treatment) to severe loss of function (high dose drug treatment). This approach contrasts with previous E-MAPs that used drugs to either induce or modify the phenotype in double-deletion mutants (Bandyopadhyay et al., 2010). Instead, interactions in our ChE-MAP result from the combined effects of a single deletion mutant and chemical inhibition of TOR kinase activity. This analysis enables characterization of the TOR signaling network due to rapid inactivation of either TORC1 or TORC2.

We used the ChE-MAP approach to provide an unbiased view of interactions with the catalytic function of the two TOR complexes. The results recapitulate known regulatory relationships between TORC2 and sphingolipid biosynthesis. Statistical analysis revealed enrichment in metabolic processes and analysis of metabolic pathways revealed an interaction network signature suggesting involvement of TORC2 in regulation the pentose phosphate pathway (PPP). Further study showed levels of key metabolites in the PPP decreased in response to TORC2 inhibition but not TORC1 inhibition, suggesting a specific and previously unappreciated role for TORC2 in regulating cellular ribosides.

Results and Discussion

A chemical-genetic tool for studying TORC2

Analog-sensitive kinases contain an active site mutation, termed the gatekeeper, that allows selective inhibition with a compound that is too bulky to fit into the active site of wild-type

kinases (Bishop et al., 2000). This residue is typically a branched chain amino acid in the hydrophobic affinity pocket within the active site of the kinase (Buzko and Shokat, 2002). Mutation to a smaller residue permits binding of the bulky inhibitor.

Based on the homology of mTOR to PI3Kγ, we performed a structure-based alignment to identify the gatekeeper residue (I2237) of *H. sapiens* mTOR (Figure 1a). Insertion of mTOR inhibitor BEZ235 into the active site guided by the affinity of backbone carbonyl of V2227 to the quinoline nitrogen (the most common mode of kinase inhibitor binding) shows a steric clash with the hydrophobic pocket that is exacerbated in the presence of other branched chain aliphatic residues such as leucine (shown). This binding mode was confirmed in the recently published structure of mTOR bound to the structurally related inhibitor Torin2 (Yang et al., 2013). In contrast, the reported wild-type TOR1/2 inhibitor in yeast, QL-IX-55 (Liu et al., 2012), containing a smaller moiety, 2-aminopyridine, in place of the quinoline moiety shows no steric clash. We reasoned that we could mutate the gatekeeper to a smaller residue in order to make space in the hydrophobic affinity pocket to accommodate a larger inhibitor. We then performed a sequence alignment to identify the conserved leucine gatekeeper in *S. cerevisiae* TOR2 (Figure 1b). The gatekeeper residue of *S. cerevisiae* TOR2 was identified as L2178, mutated to alanine, and genomically integrated into the TOR2 locus yielding cells containing as-TOR2.

Since TOR2 kinase activity is essential in *S. cerevisiae*, replacement of TOR2 with a mutant that supports viability indicates that the as-TOR2 allele is catalytically active. Nearly equivalent growth rates of wild-type and analog-sensitive (as) alleles in YPD (Figure S1A) indicate the as-TOR2 cells have a functional kinase.

Screening of the mutant kinase against a panel of ~40 ATP-analogs and kinase inhibitors (Figure S1B) revealed that the as-TOR2 allele was selectively inhibited by a single agent, BEZ235, while the growth of wt-TOR2 was relatively insensitive to this compound (Figure 1c). Although typical chemical scaffolds for inhibition of analog-sensitive kinases based on a pyrazolo-pyrimidine scaffold (Bishop et al., 2000), or compounds designed to target the gatekeeper residue of lipid kinases (Alaimo et al., 2005) showed no activity toward as-TOR2 (Figure S1C), BEZ235 (but not other compounds) also inhibited as-MEC1 suggesting this compound may be a novel and general scaffold for inhibiting as-kinases in the PIKK family.

While BEZ235 is a potent mTOR inhibitor in mammals (Maira et al., 2008), it only has activity toward wild-type yeast at high concentrations (Figure 1c, 1d) and mutation of TOR2 to the mTOR gatekeeper (isoleucine) does not confer sensitivity to the drug (Figure S2). This is likely due to slightly different positioning of the hinge loop in the mTOR kinase that pulls the quinolone moiety further from the hydrophobic pocket containing the gatekeeper residue.

In order to characterize the specificity of BEZ235 for as-TOR2, we investigated potential off target effects of the compound on kinases in the same family. We ruled out off-target effects of BEZ235 on essential kinases (MSS4 and PIK1) since these would have resulted in growth inhibition of wild-type cells. To test if BEZ235 was targeting PI3K ortholog VPS34, we made VPS34 conditionally essential in ΔTOR1 background and observed no growth

inhibition by BEZ235 (Figure S2). The compound also shows no activity toward wt-TOR1 or wt-TOR2 alleles when perturbed at high temperature or pharmacologically using rapamycin (Figure S2).

To test the selectivity of BEZ235 for as-TOR2, we measured the cellular EC50 of as-TOR2 in liquid culture. The EC50 of as-TOR2 is 189nM compared to an EC50 of 1035nM FOR wt-TOR2 (Figure 1c). Since we planned to do many experiments on agar plates, we also performed a dose series from 0.1–2.0 μM BEZ235 (Figure 1d). Results show potent inhibition of the as-TOR2 strain and only a slight growth defect in wt-TOR2 cells at the highest concentration. In order to verify that these effects were due to selective inhibition of TORC2 *in vivo*, we compared the phosphorylation of the well-characterized TORC2 substrate, YPK1, in wt-TOR2 cells and as-TOR2 cells. While phospho-YPK1 does not show significant inhibition until 4μM BEZ235 in wild-type cells, it does show significant inhibition at 0.25μM in as-TOR2 cells (Figure 1e).

To assess whether this sensitivity was due to the TOR2 kinase, we performed in vitro kinase assays using TORC2 purified (with HA-tagged TSC11, a TORC2 specific component) from cells containing as-TOR2 or wt-TOR2. The kinase assay shows the IC50 of BEZ235 for TORC2 is 50nM while the IC50 for wild-type is 111nM (Figure 1f, Figure S2). The potency was measured at 100μM ATP. Since the mutation commonly increases the Km for ATP (Zhang and Shokat, 2007), the decrease in competition with ATP would further enhance the efficacy of BEZ235 in cells.

Two potentially complicating factors in our analysis of TORC2 function through inhibition of as-TOR2 were first, the presence of TOR2 in TORC1 (Loewith et al., 2002) and second, the possibility that BEZ235 might simply inhibit TORC1 in the presence of a slightly weaker as-TOR2 allele. To test whether TOR2 was a major contributor to the activity of TORC1 and to see if BEZ235 inhibited TORC1, we purified TORC1 from as-TOR2 cells and wt-TOR2 cells. We found that the IC50 of BEZ235 for TORC1 purified from wild-type cells is 423nM. This IC50 is too weak to account for the potent growth inhibition of as-TOR2 since there is at least a 5-fold and sometimes a 100-fold shift in potency from in vitro IC50 to in vivo EC50 due to cellular competition with ATP and the poor permeability of the cell wall in yeast. This indicates BEZ235 does not inhibit TORC1, particularly at concentrations used in this study. Furthermore, the IC50 of BEZ235 for TORC1 purified from as-TOR2 containing cells (432nM) indicates that there is not significant inhibition of any as-TOR2 that may participate in TORC1 (Figure 1f, Figure S2).

Finally, to asses whether BEZ235 was inhibiting TORC1 *in vivo*, we compared the phosphorylation of the TORC1 substrate Sch9 at T737 (Urban et al., 2007) in cells containing both wt-TOR2 and as-TOR2. We did not observe a significant difference in SCH9 phosphorylation between the two strains indicating BEZ235 does not inhibit TORC1 (Figure S2), whereas rapamycin did block Sch9 phosphorylation equivalently in both wild-type and as-TOR2 cells.

To characterize genetic interactions resulting from selective inhibition of TORC1, we performed screens with the wild-type allele in the presence of rapamycin and with the as-

TOR2 allele in the presence of BEZ235. These datasets shed light on the distinct signaling networks of TORC1 and TORC2 and provides the first unbiased *and* selective investigation of genetic interactions with TORC2 kinase activity (Figure 2a).

A global map of genetic interactions with the TOR2 kinase

To systematically investigate synergistic interactions with TORC1 and TORC2, we combined our chemical-genetic tool with high-throughput yeast genetics to quantitatively assess the strength of synergistic interactions against a broad set of deleted genes. We systematically crossed either wt-TOR2 or the as-TOR2 allele with a library of ~1000 non-essential deletion mutants and selected for the haploid double mutant strains (Figure 2b). By growing strains on synthetic complete media containing either DMSO or increasing concentrations of rapamycin or BEZ235, we were able to measure dose-dependent growth phenotypes of mutant yeast colonies and use these phenotypes to compute individual genetic interaction scores. These screens were done in tandem with many other queries (Table S1) to ensure robust statistics that are required for calculation of S-scores (Collins et al., 2006; 2010; Schuldiner et al., 2006).

To evaluate the strength of the chemical-genetic interaction with either TOR complex, we computed S-scores for all observed strains. An S-score is a quantitative assessment of the strength and reproducibility of the interaction between two alleles (Collins et al., 2006; 2010). For interactions that showed a consistent *and* directional trend in correlating with drug dose, we calculated a difference score ΔS (ΔS = High Drug – DMSO). Since ΔS is a close analog to S-score, and S = 2.6 has been used previously as a cutoff for significance in published literature (Fiedler et al., 2009), we chose $\Delta S \geq |2.6|$ as a cutoff for significance in our analysis.

Three of these datasets are experimental controls for off-target effects of the compounds (Figure 2b). wt-TOR2 cells were treated with the same concentrations of BEZ235 as as-TOR2, and rapamycin resistant (rr) alleles (Cafferkey et al., 1993; Heitman et al., 1991; Helliwell et al., 1994) of TOR1 and of TOR2 (S1972I-TOR1 and S1975I-TOR2) were treated with rapamycin. The limited number of genes that showed dose-dependent interactions with the drug-resistant alleles were filtered from the experimental datasets. The two experimental datasets reveal dose-dependent genetic interactions between specific yeast genes and rapamycin or BEZ235 (Figure 2c, Table S2). The examined library of yeast genes includes genes from all functional categories, including regulatory proteins, signaling machinery, cell cycle regulators, and metabolic enzymes (Table S2).

Characteristic dose dependent ChE-MAP interactions

Analysis of ChE-MAPs generated with wild-type cells mated to deletion mutants and grown on 0, 0.25 μM, and 1 μM of BEZ235 show the compound is selective for the analog-sensitive allele with few off-target effects (Figure 2d). Only three dose-dependent genetic interactions are seen above $\Delta S \geq |2.6|$ in the wild-type dataset suggesting that our method identifies few false positives. We analyzed the distribution of S-scores for wt-TOR2 and as-TOR2 at 1μM BEZ235 (Figure 2e). Based on previous E-MAP datasets, our expectation was that wt-TOR2 would show characteristic single mutant phenotypes with S-scores at or near

zero. This phenotype should persist at all drug doses if BEZ235 is selective for as-TOR2. At the highest dose of BEZ235, we observe a clear direct relationship between S-score and ΔS in cells containing as-TOR2. In contrast, the distribution observed when 1 μM BEZ235 is applied to the wt-TOR2 is clustered around zero as expected. While the S-score is a useful reference for quantification, it does not report on dose-dependent interactions nor does it allow filtering of genetic interactions that are not due to changes in the catalytic activity of TOR. By relying on ΔS, we are able to selectively capture dose-dependent interactions.

Few dose-dependent interactions were observed in crosses with rapamycin or BEZ235 resistant alleles. The interactions observed are due to allelic effects from the resistance marker. The rr-TOR1 showed no dose-dependent genetic interactions upon drug treatment. With the rr-TOR2 allele, 7 genes showed chemical-genetic interactions above threshold (*YPL150W*, *CKA2*, *BRE1*, *YPT7*, *IPK1*, *OPI11*, *THP3*). Dose-dependent interactions with the rr-TOR2 allele arise from rapamycin inhibition of wt-TOR1 in TORC1. These results are consistent with our in vitro data that TOR1 is the primary kinase responsible for the outputs of TORC1.

Two-hundred twenty-six dose-dependent ChE-MAP interactions were identified with rapamycin and BEZ235 treatment at our cutoff of $\Delta S \geq |2.6|$. We observed 103 rapamycin-specific dose-dependent interactions and 123 TORC2-specific interactions with an overlap of 10 genes that show a dose-dependent effect with both (Figure 2f, Figure S3). Eight of these shared interactions show a dose-dependent effect that is the same whether TORC1 or TORC2 is inhibited (Figure 2g). We infer the positive interactions that arise are due either to a shared function of both complexes. The four negative interactions are compensatory with both TOR2 and TORC1. Two genes (*RAV1*, *TMA23*) show positive interactions $\Delta S > 2.6$ with TORC2 and negative interactions $\Delta S < -2.6$ with TORC1.

Relaxing our cutoff to $\Delta S \geq |2.0|$, eight additional dose-dependent interactions were identified common to both the rapamycin and BEZ235 datasets (Fig. 2g, Figure S3). Six genes (*MED1*, *BMH2*, *RPL37A*, *JJJ1*, *SPC2*, *YLR184W*) show positive interactions with TORC2 and negative interactions with TORC1. Two genes (*MKK2* and *YNL217W*) are negative with TORC2 and positive with TORC1. The network view provides a full account of dose-dependent interactions observed with each TOR complex.

Several genes that interact with both TORC1 and TORC2 play important roles in ribosomal maturation. Our results show strong positive interactions with *KNS1*, *LHP1* and *SRP40* all of which participate in tRNA processing and ribosome maturation (Figure 2g) suggesting an important role for both TORC1 and TORC2 in these processes. While the role of TORC1 in phosphorylation of ribosomal protein S6 (RPS6) via S6-kinase (S6K) is known, (Feldman et al., 2009; Richardson et al., 2004; Urban et al., 2007), the involvement of TORC2 was not appreciated until recently (Zinzalla et al., 2011). Our data support a role of TORC2 in ribosome biogenesis since two genes (*TMA23*, *JJJ1*) involved in ribosome biogenesis (Fleischer et al., 2006; Meyer et al., 2007) and a ribosomal protein (*RPL37A*) show strong positive interactions with TORC2 while simultaneously showing strong negative interactions with TORC1 (Figure 2g) indicating these genes are in a pathway with TORC2

and offering additional evidence that ribosomal biogenesis plays a role in regulating TORC2 (Zinzalla et al., 2011).

Enrichment of Sphingolipid Biosynthesis in TORC2 ChE-MAP hits

Next we looked in our datasets for well characterized signaling pathways downstream of TORC2. The sphingolipid biosynthesis pathway is the best characterized pathway under the control of TORC2 (Aronova et al., 2008; Beeler et al., 1998; Tabuchi et al., 2006). TORC2 is known to directly phosphorylate and regulate Ypk1/2 (Aronova et al., 2008; Kamada et al., 2005; Niles et al., 2012) and Ypk1/2 in turn phosphorylates and inactivates Orm1 and Orm2, which negatively regulate sphingolipid biosynthesis (Breslow et al., 2010; Niles et al., 2012; Roelants et al., 2011; Sun et al., 2012). We found extensive evidence for sphingolipid biosynthesis positively interacting with the kinase activity of TORC2 (Figure 3a).

The dose-dependent chemical genetic interactions between TORC2 and sphingolipid biosynthesis serve as a biological benchmark for the technique. We observe strong dose dependent chemical genetic interactions between TORC2 and *ORM2* (+3.4), *DPL1* (+3.9), *LCB4* (+4.2), and *ISC1* (+4.4), all of which play integral roles in the pathway (Figure 3a). No interaction is observed with TORC1, in good agreement with prior findings.

To confirm this phenotype, we performed tetrad analysis with these mutants and subjected crosses corresponding to the ChE-MAP results to increasing concentrations of rapamycin and BEZ in a spot dilution assay (Figure 3b). The results show that Orm2 shows a positive phenotype upon TORC2 inhibition. The positive genetic interactions with several members of the sphingolipid biosynthesis pathway validate the ChE-MAP as a viable strategy for identification of downstream signaling pathways.

Cellular Compartment and Process Enrichment of TORC2 Interactions

Using the ChE-MAP interaction data, we asked whether there was functional enrichment for genes annotated in a particular cellular compartment or biological process. Our results were not biased since we included a diverse and balanced collection of queries in the ChE-MAP (Figure 3c).

TORC2 interacting genes were analyzed for gene ontology (GO) (Berriz et al., 2009) terms for cellular compartment showed a two-fold enrichment for proteins that localize to the endoplasmic reticulum ($p < 0.05$), controlling for sampling bias in the gene deletion library used for this study. This result is consistent with recent work showing mammalian TORC2 co-fractionates with the ER (Boulbés et al., 2011), suggesting the localization of TORC2 is conserved and expands our understanding of previous work showing TORC2 in *S. cerevisiae* localizes to the plasma membrane and regulates sphingolipid biosynthesis (Berchtold and Walther, 2009; Berchtold et al., 2012). TORC1, by contrast, localizes in the vacuole of *S. cerevisiae* and to the lysosome surface in mammalian cells (Berchtold and Walther, 2009; Loewith et al., 2002; Zoncu et al., 2011).

Next, we analyzed the TORC1 and TORC2 datasets for enrichment of hits mapping to specific biological processes (Berriz et al., 2009). While no significant enrichment was

observed with TORC1 hits, significant enrichment was observed for positive hits with TORC2. The ChE-MAP showed significant enrichment ($p < 0.05$) for 'generation of precursor metabolites and energy' for positively interacting TORC2 hits. While TOR has been loosely associated with energy homeostasis due to the obvious energetic demands of protein synthesis and ribosome biogenesis, a link with metabolite synthesis was not previously shown. To investigate this further, we sought to integrate published physical interaction data with our chemical genetic results to see if there were specific metabolic processes with predominantly positive interactions with TORC2.

Integrated functional network of TOR signaling

To look for proteins involved in metabolite synthesis that physically interact with TOR, we searched for genes in metabolic GO terms that had large numbers of physical interactions with members of the TOR signaling pathway. We found that many proteins in the pentose phosphate pathway (PPP) have physical interactions with proteins in the TOR signaling pathway compelling us to construct a comprehensive network of PPP proteins that physically interact with each of the TOR complexes.

The network of genes that are annotated (by GO terms) to the PPP shows a distinct signature with TORC1 genes compared with TORC2 genes (Figure 4a). The figure shows that many enzymes that catalyze steps in the PPP physically interact with proteins that positively interact with as-TOR2 (*BDF2*, *GAC1*, *URN1*, *YPL150W*). In contrast, enzymes in the PPP generally show physical interactions with proteins that negatively interact with TORC1 (*TPM1*, *SET2*, *HAT2*). The network shows greater than 2-fold enrichment of positive interactions with TORC2 above what would be expected by chance alone (p-value = 0.02) and predominantly negative interactions with TORC1 (p-value not significant), suggesting the PPP is in a linear pathway with TORC2, and either in a non-interacting or parallel pathway to TORC1. This phenotype is the hallmark of a TORC2 regulated pathway and motivated us to investigate whether metabolite levels and particularly the PPP was regulated by TORC2.

Metabolomic analysis of TORC1 and as-TOR2

To test the role of TORC2 in the PPP, we used reverse-phase ion-paired LC/MS to monitor drug dependent changes to over ~130 cellular metabolites including constituents of the PPP pathway (Figure S4). Rapid metabolic changes that take place soon after drug treatment suggest direct regulation of metabolic enzymes while changes that occur on the timescale of yeast cell replication/division are more likely to indicate transcriptional changes to metabolic enzymes.

As an internal quantitative and qualitative reference for the magnitude of the metabolic changes and a point of comparison for our drug treatment, we also assessed metabolic changes due to nitrogen starvation. Nitrogen-starvation is akin to rapamycin in that it disrupts phosphorylation of TORC1 substrates (Urban et al., 2007). To identify changes to metabolite levels in response to inhibition of the TOR kinase, cells were treated with inhibitors or switched to low-nitrogen media and metabolic changes were quantified over time by LC/MS to look for inhibitor dependent changes in soluble metabolite levels.

Inhibition of TORC1 or TORC2 leads to broad changes across all aspects of metabolism. We filtered the metabolic results to capture the change in response upon drug inhibition over the 60 minute time-course. After 1 hour of drug treatment, above a threshold of log(metabolite) ≥ |1.5|, nitrogen-starvation shows changes in 18 metabolites out of 128 measured, rapamycin shows changes in 24 metabolites out of 128 measured, while TORC2 treatment affects 19 out of 114 metabolites measured.

We observed that metabolic intermediates involved in the PPP are strongly downregulated in response to as-TOR2 inhibition. In our experiments 6-phospho-D-gluconate (6PG) and ribose-5-phosphate (R5P), two intermediates that are specific to the PPP, show a rapid time-dependent response to treatment with BEZ235 (Figure 4b, 4c) but slower and more modest response to rapamycin. R5P is the product of the oxidative pentose phosphate pathway and was recently shown to be produced by riboneogenesis (Clasquin et al., 2011). While this metabolite is perturbed due to the as-TOR2 allele, the metabolite shows and additional time-dependent decrease in levels after 7 minutes of treatment with BEZ235. These changes may suggest a role for TORC2 in regulating both the oxidative and non-oxidative branches of the PPP.

In contrast, the delayed down-regulation in response to TORC1 inhibition is consistent with previously proposed models that put enzymes in the PPP under the control of transcription factors downstream of TORC1 (Düvel et al., 2010; Robitaille et al., 2013). The rapid response upon BEZ235 treatment indicates that TORC2 may have more direct control over the PPP through kinase signaling. This hypothesis is supported by GO analysis of the ChE-MAP (Figure 4a) that shows seven proteins with chemical-genetic interactions with TORC2 are annotated to physically interact with metabolic enzymes of the PPP. All of these are positive interactions indicating they are in a linear pathway with TORC2. Strong positive interactors with TORC2 include *BDF2* and *GAC1*, which both physically interact with tRNA export protein Sol1, a close homolog of Sol3/Sol4 that catalyze the second step of the PPP leading to the generation of 6PG. Strong interactions are also observed between TORC2 and *RBL2* which physically interacts with Rki1. Rki1 regulates the third step in the PPP leading to the production R5P.

To test whether TORC2 was influencing metabolite levels in the PPP by direct regulation of metabolic flux, we undertook analysis of using the tracer 1,2-^{13}C-glucose to quantify levels of 6PG and R5P and to measure the relative ratio of oxidative PPP and non-oxidative PPP transketolase reaction. The rapid decrease of 6PG in the as-TOR2 strain upon BEZ235 addition (Figure 4d) confirms TORC2's posttranslational regulation of the oxidative PPP since the change in metabolite levels occurs on a rapid timescale (< 30 minutes) as previously observed. The lack of substantial change of oxidative PPP flux in the as-TOR2 strain relative to wild-type (Figure S4) upon BEZ235 treatment suggests TORC2 does not differentially regulate the oxidative and non-oxidative PPP, and may regulate the PPP upstream of the split between the oxPPP and non-oxPPP, likely through differential regulation of glucose-6-phosphate dehydrogenase (the reaction upstream of 6-phosphogluconate) and 6-phosphogluconate dehydrogenase.

Conclusions

Yeast screens remain the most versatile tool for assessing functional genomic interactions at the organismal level. Genetic knockouts are facile for non-essential genes, but other methods are required for queries of essential genes such as the TOR2 kinase. Among these, decreased abundance by mRNA perturbation (DAmP), temperature-sensitive degrons designed to rapidly degrade proteins at the restrictive temperature, or chemical inhibitors for a specific target are the most commonly employed techniques. Use of DAmP alleles can be unreliable due to variable levels of knockdown. Temperature-sensitive (ts) strategies are effective but can suffer from pleiotropy. In particular, several different TOR2-ts isolates have been reported to have widely varying effects on cell cycle, budding, and actin structures at the restrictive temperature (Helliwell et al., 1998a). Chemical inhibitors are fast-acting, but the number of interesting essential targets far exceeds existing chemical tools to inhibit them.

In this study, we created a chemical-genetic tool that is highly specific and allows rapid inactivation of the TORC2 kinase. We used this tool to systematically and quantitatively probe the genetic interaction landscape of TORC2 kinase activity *in vivo*. Our method reports precisely on *kinase activity* and avoids the plethora of interactions that arise from destruction of protein/protein interactions.

We confirmed the robustness of our technique through positive identification of the sphingolipid biosynthesis pathway downstream of TORC2 and show a significant enrichment in functional connections with proteins localized to the endoplasmic reticulum. Data showing enrichment for ‘generation of metabolites and energy’ directed us to investigate the PPP with physical interaction networks that showed a pattern of interactions that is consistent with the PPP existing in a linear pathway with TORC2. By studying metabolite levels with as-TOR2 in the presence of BEZ, we were able to observe large and rapid (< 30 min) changes in metabolites that are created in the PPP and further showed these changes necessarily occur upstream of the transketolase reaction since data does not suggest a differential flux through the non-oxidative and oxidative PPP.

The suggestion of a role for TORC2 in ribosomal biogenesis (Figure 2e) has interesting implications for how the cell balances energy demands to meet these needs. Emerging evidence indicates TORC2 is an important node in ribosome biogenesis (Zinzalla et al., 2011). The high energy requirements of ribosome biogenesis creates high demand for ribose relative to NADPH leading to activation of the PPP and production of R5P (Clasquin et al., 2011). Our evidence shows that TORC2 positively regulates metabolite synthesis in the PPP (Figure 4d), and may act as a critical relay between ribosome biogenesis and the PPP. This is particularly compelling in conjunction with evidence showing that upregulation of the non-oxidative PPP is required for tumor survival (Deberardinis et al., 2008).

Our approach represents a unique union of genetics and pharmacology that facilitates rapid assessment of gene selective effects that could act as a first line of evidence in the search for synergistic therapeutics. It allows for a more granular analysis of functional genetic interactions that refer specifically to the *catalytic activity* of the kinase rather than

scaffolding roles of the Tor protein. These findings will be a valuable resource for deciphering the different physiological functions of TORC1 and TORC2 in yeast. Such understanding in turn may help understand the roles these complexes play in mammals, where this approach cannot be directly applied, and thereby aid in the design of combination therapy regimens involving TOR inhibitors.

Experimental Procedures

Generation of point mutants

The C-terminal region TOR1 or TOR2 (including the FAT, FRB, kinase domain, and 160 bp of 3′UTR) was cloned onto plasmid pFA6-NAT-MX6, into the multiple cloning site immediately preceding the NAT gene (which confers resistance to Nourseothricin, Werner Bioagents). as-TOR2 (L2178A), rr-TOR2 (S1975I), and rr-TOR1 (S1972I) mutants were generated using site directed mutagenesis. These mutants were amplified using PCR and transformed into the BY4742 strain, in which the C-terminal region of either TOR1 or TOR2 had been displaced by k.l URA3. Following selection on NAT and 5-FOA, the mutants were sequenced to confirm insertion of the desired mutations. Subsequently, the diploid mutant strains were sporulated and the Matα haploid strains were selected for as described previously, and presence of the mutation was again confirmed by sequencing.

E-MAP experiments

Strain construction, plating of mutants, mutant selection, and scoring of genetic interactions (S-scores) were performed as previously described (Collins et al., 2006; Schuldiner et al., 2005). Using a Singer Instruments pinning robot, haploid double mutants were simultaneously grown in 1536-well format at 30 degrees Celsius on agar plates containing DMSO or containing a selective TOR inhibitor. Mutants in this study were screened in tandem with a large number of queries (Table S4) to ensure robust statistics for averaging ($n > 30$). Several unrelated queries, strains containing point mutants to SCH9, wild-type strains containing a TOR1 marker, a ts-TOR2 allele were used as query strains. For the plates containing inhibitor, 0.25μM BEZ235, 1.00μM BEZ235, 10nM rapamycin, or 100nM rapamycin were added to the plates containing selective media. Plates were photographed and the area of each colony was converted into pixels to quantitatively assess colony size. In untreated or treated conditions, colony sizes were based on 3 replicate measurements. For a given double mutant, the experimental data was used to assign a quantitative S-score based on a modified T-test that compares the observed double mutant growth rate to an expected growth rate based on the average colony size across an entire plate.

Dose-dependent interaction scoring system

Dose-dependent genetic interactions were identified for a given gene by searching for a series of S-scores for that gene that show a directional shift that correlates with drug concentration. The magnitude of the interaction was evaluated as the difference between the high-dose and the control strain ($\Delta S = \text{S-score}_{\text{highdrug}} - \text{S-score}_{\text{DMSO}}$). ΔS-scores ≥ |2.6|.

Cellular compartment enrichment of TORC2 dose-dependent interactions

Enrichment of TORC2 dose-dependent interactions: Genes with a dose-dependent interaction $\Delta S \geq |2.0|$ were tested for enrichment in a specific cellular compartment. A Fisher's exact test (Berriz et al., 2009) was used to identify terms in the cellular compartment GO Slim that were significantly enriched in dose-dependent hits, resulting in the observation that dose-dependent hits are ~1.6 times more likely to be localized to the endoplasmic reticulum than expected ($p < 0.05$ after correcting for multiple testing). The background for this calculation was all mutants with measured scores from the as-TOR2 + BEZ235 screen, and consequently the observed enrichment is not due to the bias on the array, or due to data quality filtering. The same approach was used to identify terms in the Biological Process Ontology showing significant enrichment for dose-dependent. All process terms having 1.5-fold or better enrichment are shown in Figure 3.

Tetrad Analysis

wt-TOR2 and as-TOR2 were mated to a single delete (SD) strain of interest for 48 hours prior to sporulation at room temp for 3–5 days. Digested ascus with zymolyase for 20min prior to tetrad dissection. Replica plated tetrads on selective media for genotyping and verified all strains using check PCR and sequencing of the TOR kinase domain locus.

Spot Test Assay

Overnight cultures were grown to saturation, diluted to OD_{600}= 0.2 and grew until all four strains were OD_{600}= 0.8. 2-fold serial dilutions of cells were plated on DMSO, 0.1μM, 0.25μM, and 1μM BEZ235 or on 10nM 50nM, 100nM rapamycin. Plates were grown at 30°C and imaged after 24h.

Gene Ontology Network Analysis

Circular nodes were created for all genes within a given GO term. Then, rectangular nodes were generated for hits in either the rapamycin or BEZ235 datasets and were linked to the circular nodes based literature reported physical interactions (Stark et al., 2006). Genetic interactions between TORC1 or as-TOR2 computed and illustrated using blue edges.

Metabolite Measurement—The metabolome of *Saccharomyces cerevisiae* was characterized as described previously (Xu et al., 2012). Saturated overnight cultures were diluted 1:30 and grown in liquid media in a shaking flask to A600 of ~ 0.6. A portion of the cells (3 mL) were filtered onto a 50 mm nylon membrane filter, which was immediately transferred into −20°C extraction solvent (40:40:20 acetonitrile/methanol/water). Serial extraction was then carried out at indicated time points after drug treatment. Cell extracts were analyzed by reversed phase ion-pairing liquid chromatography (LC) coupled by negative-mode electrospray ionization (ESI) to a high-resolution, high-accuracy mass spectrometer (Exactive; Thermo Fisher Scientific) operated in full scan mode at 1 s scan time, 10^5 resolution, with compound identities verified by exact mass and retention time matched to an authenticated standard (Melamud et al., 2010). Isomers are reported separately only where they fully chromatographically resolved.

Metabolic Flux Measurement—Yeast cells were grown in 1,2-$^{13}C_2$-glucose in the presence of 1 nM or 5 nM estradiol. The use of 1,2-^{13}C-glucose allows measurement of oxidative pentose phosphate pathway flux. All the isotope-labeled forms of ribose phosphate are quantitated. The flux is calculated as following: Oxidative pentose phosphate pathway flux = $(f_1 + f_2)/(f_3 + f_4 – f_0)$ in which f_n is the labeling fraction of the n-labeled ribose phosphate. The oxidative branch of the pentose phosphate pathway yields 1- and 3-labeled pentose phosphate. The non-oxidative branch of the pentose phosphate pathway yields 2- and 4-labeled pentose phosphate. One molecule of 0-labeled pentose phosphate is generated for every 2- or 4-labeled pentose phosphate produced through erythrose phosphate. Therefore 0-labeled pentose phosphate is subtracted to reflect the true flux of non-oxidative pentose phosphate pathway.

Supplementary Material

Refer to Web version on PubMed Central for supplementary material.

Acknowledgments

The authors thank A. Roguev, H. Braberg, J. Lipp, G. Ducker and members of the Krogan and Shokat labs for helpful comments and discussions. The work was supported by the National Science Foundation (J.I.K.), the Irish Research Council (C.J.R), the Howard Hughes Medical Institute (K.M.S.), the NIH (N.J.K. GM084448, GM084279, GM081879 and GM098101 and K.M.S.), and the Sandler Family Foundation (N.J.K.). N.J.K. is a Searle Scholar and a Keck Young Investigator.

Bibliography

Alaimo PJ, Knight ZA, Shokat KM. Targeting the gatekeeper residue in phosphoinositide 3-kinases. Bioorg Med Chem. 2005; 13:2825–2836. [PubMed: 15781393]

Aronova S, Wedaman K, Aronov PA, Fontes K, Ramos K, Hammock BD, Powers T. Regulation of ceramide biosynthesis by TOR complex 2. Cell Metab. 2008; 7:148–158. [PubMed: 18249174]

Bandyopadhyay S, Mehta M, Kuo D, Sung MK, Chuang R, Jaehnig EJ, Bodenmiller B, Licon K, Copeland W, Shales M, et al. Rewiring of genetic networks in response to DNA damage. Science. 2010; 330:1385–1389. [PubMed: 21127252]

Beeler T, Bacikova D, Gable K, Hopkins L, Johnson C, Slife H, Dunn T. The Saccharomyces cerevisiae TSC10/YBR265w gene encoding 3-ketosphinganine reductase is identified in a screen for temperature-sensitive suppressors of the Ca2+-sensitive csg2Delta mutant. J Biol Chem. 1998; 273:30688–30694. [PubMed: 9804843]

Beltrao P, Cagney G, Krogan NJ. Quantitative genetic interactions reveal biological modularity. Cell. 2010; 141:739–745. [PubMed: 20510918]

Berchtold D, Walther TC. TORC2 plasma membrane localization is essential for cell viability and restricted to a distinct domain. Mol Biol Cell. 2009; 20:1565–1575. [PubMed: 19144819]

Berchtold D, Piccolis M, Chiaruttini N, Riezman I, Riezman H, Roux A, Walther TC, Loewith R. Plasma membrane stress induces relocalization of Slm proteins and activation of TORC2 to promote sphingolipid synthesis. Nat Cell Biol. 2012; 14:542–547. [PubMed: 22504275]

Berriz GF, Beaver JE, Cenik C, Tasan M, Roth FP. Next generation software for functional trend analysis. Bioinformatics. 2009; 25:3043–3044. [PubMed: 19717575]

Bishop AC, Ubersax JA, Petsch DT, Matheos DP, Gray NS, Blethrow J, Shimizu E, Tsien JZ, Schultz PG, Rose MD, et al. A chemical switch for inhibitor-sensitive alleles of any protein kinase. Nature. 2000; 407:395–401. [PubMed: 11014197]

Boss DS, Beijnen JH, Schellens JHM. Clinical experience with aurora kinase inhibitors: a review. Oncologist. 2009; 14:780–793. [PubMed: 19684075]

Boulbés DR, Shaiken T, Sarbassov DD. Endoplasmic reticulum is a main localization site of mTORC2. Biochem Biophys Res Commun. 2011; 413:46–52. [PubMed: 21867682]

Breslow DK, Cameron DM, Collins SR, Schuldiner M, Stewart-Ornstein J, Newman HW, Braun S, Madhani HD, Krogan NJ, Weissman JS. A comprehensive strategy enabling high-resolution functional analysis of the yeast genome. Nat Methods. 2008; 5:711–718. [PubMed: 18622397]

Breslow DK, Collins SR, Bodenmiller B, Aebersold R, Simons K, Shevchenko A, Ejsing CS, Weissman JS. Orm family proteins mediate sphingolipid homeostasis. Nature. 2010; 463:1048–1053. [PubMed: 20182505]

Buzko O, Shokat KM. A kinase sequence database: sequence alignments and family assignment. Bioinformatics. 2002; 18:1274–1275. [PubMed: 12217924]

Cafferkey R, Young PR, McLaughlin MM, Bergsma DJ, Koltin Y, Sathe GM, Faucette L, Eng WK, Johnson RK, Livi GP. Dominant missense mutations in a novel yeast protein related to mammalian phosphatidylinositol 3-kinase and VPS34 abrogate rapamycin cytotoxicity. Mol Cell Biol. 1993; 13:6012–6023. [PubMed: 8413204]

Casadio A, Martin KC, Giustetto M, Zhu H, Chen M, Bartsch D, Bailey CH, Kandel ER. A transient, neuron-wide form of CREB-mediated long-term facilitation can be stabilized at specific synapses by local protein synthesis. Cell. 1999; 99:221–237. [PubMed: 10535740]

Clasquin MF, Melamud E, Singer A, Gooding JR, Xu X, Dong A, Cui H, Campagna SR, Savchenko A, Yakunin AF, et al. Riboneogenesis in yeast. Cell. 2011; 145:969–980. [PubMed: 21663798]

Collins SR, Miller KM, Maas NL, Roguev A, Fillingham J, Chu CS, Schuldiner M, Gebbia M, Recht J, Shales M, et al. Functional dissection of protein complexes involved in yeast chromosome biology using a genetic interaction map. Nature. 2007; 446:806–810. [PubMed: 17314980]

Collins SR, Roguev A, Krogan NJ. Quantitative genetic interaction mapping using the E-MAP approach. Meth Enzymol. 2010; 470:205–231. [PubMed: 20946812]

Collins SR, Schuldiner M, Krogan NJ, Weissman JS. A strategy for extracting and analyzing large-scale quantitative epistatic interaction data. Genome Biol. 2006; 7:R63. [PubMed: 16859555]

Deberardinis RJ, Sayed N, Ditsworth D, Thompson CB. Brick by brick: metabolism and tumor cell growth. Curr Opin Genet Dev. 2008; 18:54–61. [PubMed: 18387799]

Düvel K, Yecies JL, Menon S, Raman P, Lipovsky AI, Souza AL, Triantafellow E, Ma Q, Gorski R, Cleaver S, et al. Activation of a metabolic gene regulatory network downstream of mTOR complex 1. Mol Cell. 2010; 39:171–183. [PubMed: 20670887]

Fan X, Martin-Brown S, Florens L, Li R. Intrinsic capability of budding yeast cofilin to promote turnover of tropomyosin-bound actin filaments. PLoS ONE. 2008; 3:e3641. [PubMed: 18982060]

Fasolo J, Sboner A, Sun MGF, Yu H, Chen R, Sharon D, Kim PM, Gerstein M, Snyder M. Diverse protein kinase interactions identified by protein microarrays reveal novel connections between cellular processes. Genes Dev. 2011; 25:767–778. [PubMed: 21460040]

Feldman ME, Apsel B, Uotila A, Loewith R, Knight ZA, Ruggero D, Shokat KM, Hunter T. Active-Site Inhibitors of mTOR Target Rapamycin-Resistant Outputs of mTORC1 and mTORC2. PLoS Biol. 2009; 7:e38. [PubMed: 19209957]

Fiedler D, Braberg H, Mehta M, Cagney G, Shales M, Collins SR, et al. Functional organization of the S. cerevisiae phosphorylation network. Cell. 2009; 136:952–963. [PubMed: 19269370]

Fleischer TC, Weaver CM, McAfee KJ, Jennings JL, Link AJ. Systematic identification and functional screens of uncharacterized proteins associated with eukaryotic ribosomal complexes. Genes Dev. 2006; 20:1294–1307. [PubMed: 16702403]

Graille M, Meyer P, Leulliot N, Sorel I, Janin J, Van Tilbeurgh H, Quevillon-Cheruel S. Crystal structure of the S. cerevisiae D-ribose-5-phosphate isomerase: comparison with the archaeal and bacterial enzymes. Biochimie. 2005; 87:763–769. [PubMed: 16054529]

Greenman C, Stephens P, Smith R, Dalgliesh GL, Hunter C, Bignell G, Davies H, Teague J, Butler A, Stevens C, et al. Patterns of somatic mutation in human cancer genomes. Nature. 2007; 446:153–158. [PubMed: 17344846]

Haura EB, Ricart AD, Larson TG, Stella PJ, Bazhenova L, Miller VA, Cohen RB, Eisenberg PD, Selaru P, Wilner KD, et al. A phase II study of PD-0325901, an oral MEK inhibitor, in previously treated patients with advanced non-small cell lung cancer. Clin Cancer Res. 2010; 16:2450–2457. [PubMed: 20332327]

Heitman J, Movva NR, Hall MN. Targets for cell cycle arrest by the immunosuppressant rapamycin in yeast. Science. 1991; 253:905–909. [PubMed: 1715094]

Helliwell SB, Howald I, Barbet N, Hall MN. TOR2 is part of two related signaling pathways coordinating cell growth in Saccharomyces cerevisiae. Genetics. 1998a; 148:99–112. [PubMed: 9475724]

Helliwell SB, Schmidt A, Ohya Y, Hall MN. The Rho1 effector Pkc1, but not Bni1, mediates signalling from Tor2 to the actin cytoskeleton. Curr Biol. 1998b; 8:1211–1214. [PubMed: 9811607]

Helliwell SB, Wagner P, Kunz J, Deuter-Reinhard M, Henriquez R, Hall MN. TOR1 and TOR2 are structurally and functionally similar but not identical phosphatidylinositol kinase homologues in yeast. Mol Biol Cell. 1994; 5:105–118. [PubMed: 8186460]

Hesselberth JR, Miller JP, Golob A, Stajich JE, Michaud GA, Fields S. Comparative analysis of Saccharomyces cerevisiae WW domains and their interacting proteins. Genome Biol. 2006; 7:R30. [PubMed: 16606443]

Inoki K, Corradetti MN, Guan KL. Dysregulation of the TSC-mTOR pathway in human disease. Nat Genet. 2005; 37:19–24. [PubMed: 15624019]

Kaeberlein M, Hu D, Kerr EO, Tsuchiya M, Westman EA, Dang N, Fields S, Kennedy BK. Increased life span due to calorie restriction in respiratory-deficient yeast. PLoS Genet. 2005; 1:e69. [PubMed: 16311627]

Kamada Y, Fujioka Y, Suzuki NN, Inagaki F, Wullschleger S, Loewith R, Hall MN, Ohsumi Y. Tor2 directly phosphorylates the AGC kinase Ypk2 to regulate actin polarization. Mol Cell Biol. 2005; 25:7239–7248. [PubMed: 16055732]

Kelley R, Ideker T. Systematic interpretation of genetic interactions using protein networks. Nat Biotechnol. 2005; 23:561–566. [PubMed: 15877074]

Knight ZA, Lin H, Shokat KM. Targeting the cancer kinome through polypharmacology. 2010:1–8.

Krogan NJ, Cagney G, Yu H, Zhong G, Guo X, Ignatchenko A, Li J, Pu S, Datta N, Tikuisis AP, et al. Global landscape of protein complexes in the yeast Saccharomyces cerevisiae. Nature. 2006; 440:637–643. [PubMed: 16554755]

Liu Q, Ren T, Fresques T, Oppliger W, Niles BJ, Hur W, Sabatini DM, Hall MN, Powers T, Gray NS. Selective ATP-Competitive Inhibitors of TOR Suppress Rapamycin-Insensitive Function of TORC2 in Saccharomyces cerevisiae. ACS Chem Biol. 2012; 7:982–987. [PubMed: 22496512]

Loewith R, Jacinto E, Wullschleger S, Lorberg A, Crespo JL, Bonenfant D, Oppliger W, Jenoe P, Hall MN. Two TOR complexes, only one of which is rapamycin sensitive, have distinct roles in cell growth control. Mol Cell. 2002; 10:457–468. [PubMed: 12408816]

Maira S-M, Stauffer F, Brueggen J, Furet P, Schnell C, Fritsch C, Brachmann S, Chène P, De Pover A, Schoemaker K, et al. Identification and characterization of NVP-BEZ235, a new orally available dual phosphatidylinositol 3-kinase/mammalian target of rapamycin inhibitor with potent in vivo antitumor activity. Mol Cancer Ther. 2008; 7:1851–1863. [PubMed: 18606717]

Martin DE, Hall MN. The expanding TOR signaling network. Curr Opin Cell Biol. 2005; 17:158–166. [PubMed: 15780592]

Melamud E, Vastag L, Rabinowitz JD. Metabolomic analysis and visualization engine for LC-MS data. Anal Chem. 2010; 82:9818–9826. [PubMed: 21049934]

Mestres J, Gregori-Puigjané E, Valverde S, Solé RV. The topology of drug-target interaction networks: implicit dependence on drug properties and target families. Mol Biosyst. 2009; 5:1051–1057. [PubMed: 19668871]

Meyer AE, Hung NJ, Yang P, Johnson AW, Craig EA. The specialized cytosolic J-protein, Jjj1, functions in 60S ribosomal subunit biogenesis. Proc Natl Acad Sci USA. 2007; 104:1558–1563. [PubMed: 17242366]

Niles BJ, Mogri H, Hill A, Vlahakis A, Powers T. Plasma membrane recruitment and activation of the AGC kinase Ypk1 is mediated by target of rapamycin complex 2 (TORC2) and its effector proteins Slm1 and Slm2. Proc Natl Acad Sci USA. 2012; 109:1536–1541. [PubMed: 22307609]

Ptacek J, Devgan G, Michaud G, Zhu H, Zhu X, Fasolo J, Guo H, Jona G, Breitkreutz A, Sopko R, et al. Global analysis of protein phosphorylation in yeast. Nature. 2005; 438:679–684. [PubMed: 16319894]

Richardson CJ, Bröenstrup M, Fingar DC, Jülich K, Ballif BA, Gygi S, Blenis J. SKAR is a specific target of S6 kinase 1 in cell growth control. Curr Biol. 2004; 14:1540–1549. [PubMed: 15341740]

Robitaille AM, Christen S, Shimobayashi M, Cornu M, Fava LL, Moes S, Prescianotto-Baschong C, Sauer U, Jenoe P, Hall MN. Quantitative Phosphoproteomics Reveal mTORC1 Activates de Novo Pyrimidine Synthesis. Science. 2013

Roelants FM, Breslow DK, Muir A, Weissman JS, Thorner J. Protein kinase Ypk1 phosphorylates regulatory proteins Orm1 and Orm2 to control sphingolipid homeostasis in Saccharomyces cerevisiae. 2011; 108:19222–19227.

Roelants FM, Torrance PD, Thorner J. Differential roles of PDK1- and PDK2-phosphorylation sites in the yeast AGC kinases Ypk1, Pkc1 and Sch9. Microbiology. 2004; 150:3289–3304. [PubMed: 15470109]

Roguev A, Bandyopadhyay S, Zofall M, Zhang K, Fischer T, Collins SR, Qu H, Shales M, Park HO, Hayles J, et al. Conservation and rewiring of functional modules revealed by an epistasis map in fission yeast. Science. 2008; 322:405–410. [PubMed: 18818364]

Ryan CJ, Roguev A, Patrick K, Xu J, Jahari H, Tong Z, Beltrao P, Shales M, Qu H, Collins SR, et al. Hierarchical modularity and the evolution of genetic interactomes across species. Mol Cell. 2012; 46:691–704. [PubMed: 22681890]

Schmidt A, Bickle M, Beck T, Hall MN. The yeast phosphatidylinositol kinase homolog TOR2 activates RHO1 and RHO2 via the exchange factor ROM2. Cell. 1997; 88:531–542. [PubMed: 9038344]

Schuldiner M, Collins SR, Thompson NJ, Denic V, Bhamidipati A, Punna T, Ihmels J, Andrews B, Boone C, Greenblatt JF, et al. Exploration of the function and organization of the yeast early secretory pathway through an epistatic miniarray profile. Cell. 2005; 123:507–519. [PubMed: 16269340]

Schuldiner M, Collins SR, Weissman JS, Krogan NJ. Quantitative genetic analysis in Saccharomyces cerevisiae using epistatic miniarray profiles (E-MAPs) and its application to chromatin functions. Methods. 2006; 40:344–352. [PubMed: 17101447]

Stark C, Breitkreutz BJ, Reguly T, Boucher L, Breitkreutz A, Tyers M. BioGRID: a general repository for interaction datasets. Nucleic Acids Res. 2006; 34:D535–D539. [PubMed: 16381927]

Sun Y, Miao Y, Yamane Y, Zhang C, Shokat KM, Takematsu H, Kozutsumi Y, Drubin DG. Orm protein phosphoregulation mediates transient sphingolipid biosynthesis response to heat stress via the Pkh-Ypk and Cdc55-PP2A pathways. Mol Biol Cell. 2012; 23:2388–2398. [PubMed: 22535525]

Tabuchi M, Audhya A, Parsons AB, Boone C, Emr SD. The phosphatidylinositol 4,5-biphosphate and TORC2 binding proteins Slm1 and Slm2 function in sphingolipid regulation. Mol Cell Biol. 2006; 26:5861–5875. [PubMed: 16847337]

Tee AR, Blenis J. mTOR, translational control and human disease. Semin Cell Dev Biol. 2005; 16:29–37. [PubMed: 15659337]

Creighton CJ, Morgan M, Gunaratne PH, Wheeler DA, Gibbs RA, Gordon Robertson A, Chu A, et al. The Cancer Genome Atlas Research Network, Analysis working group: Baylor College of Medicine; BC Cancer Agency. Comprehensive molecular characterization of clear cell renal cell carcinoma. Nature. 2013

Tischmeyer W, Schicknick H, Kraus M, Seidenbecher CI, Staak S, Scheich H, Gundelfinger ED. Rapamycin-sensitive signalling in long-term consolidation of auditory cortex-dependent memory. Eur J Neurosci. 2003; 18:942–950. [PubMed: 12925020]

Tong AHY, Lesage G, Bader GD, Ding H, Xu H, Xin X, Young J, Berriz GF, Brost RL, Chang M, et al. Global mapping of the yeast genetic interaction network. Science. 2004; 303:808–813. [PubMed: 14764870]

Urban J, Soulard A, Huber A, Lippman S, Mukhopadhyay D, Deloche O, Wanke V, Anrather D, Ammerer G, Riezman H, et al. Sch9 Is a Major Target of TORC1 in Saccharomyces cerevisiae. Mol Cell. 2007; 26:663–674. [PubMed: 17560372]

Wood LD, Parsons DW, Jones S, Lin J, Sjöblom T, Leary RJ, Shen D, Boca SM, Barber T, Ptak J, et al. The genomic landscapes of human breast and colorectal cancers. Science. 2007; 318:1108–1113. [PubMed: 17932254]

Xu YF, Zhao X, Glass DS, Absalan F, Perlman DH, Broach JR, Rabinowitz JD. Regulation of yeast pyruvate kinase by ultrasensitive allostery independent of phosphorylation. Mol Cell. 2012; 48:52–62. [PubMed: 22902555]

Yang H, Rudge DG, Koos JD, Vaidialingam B, Yang HJ, Pavletich NP. mTOR kinase structure, mechanism and regulation. Nature. 2013; 497:217–223. [PubMed: 23636326]

Yu H, Braun P, Yildirim MA, Lemmens I, Venkatesan K, Sahalie J, Hirozane-Kishikawa T, Gebreab F, Li N, Simonis N, et al. High-quality binary protein interaction map of the yeast interactome network. Science. 2008; 322:104–110. [PubMed: 18719252]

Zhang C, Shokat KM. Enhanced selectivity for inhibition of analog-sensitive protein kinases through scaffold optimization. Tetrahedron. 2007; 63:5832–5838.

Zinzalla V, Stracka D, Oppliger W, Hall MN. Activation of mTORC2 by association with the ribosome. Cell. 2011; 144:757–768. [PubMed: 21376236]

Zoncu R, Bar-Peled L, Efeyan A, Wang S, Sancak Y, Sabatini DM. mTORC1 senses lysosomal amino acids through an inside-out mechanism that requires the vacuolar H(+)-ATPase. Science. 2011; 334:678–683. [PubMed: 22053050]

Highlights

1. Selective pharmacology of TORC2
2. A Chemical-Genetic Epistasis Map Differentiates Between TORC1 and TORC2 Pathways
3. First Evidence TORC2 inhibition rapidly regulates the Pentose Phosphate Pathway

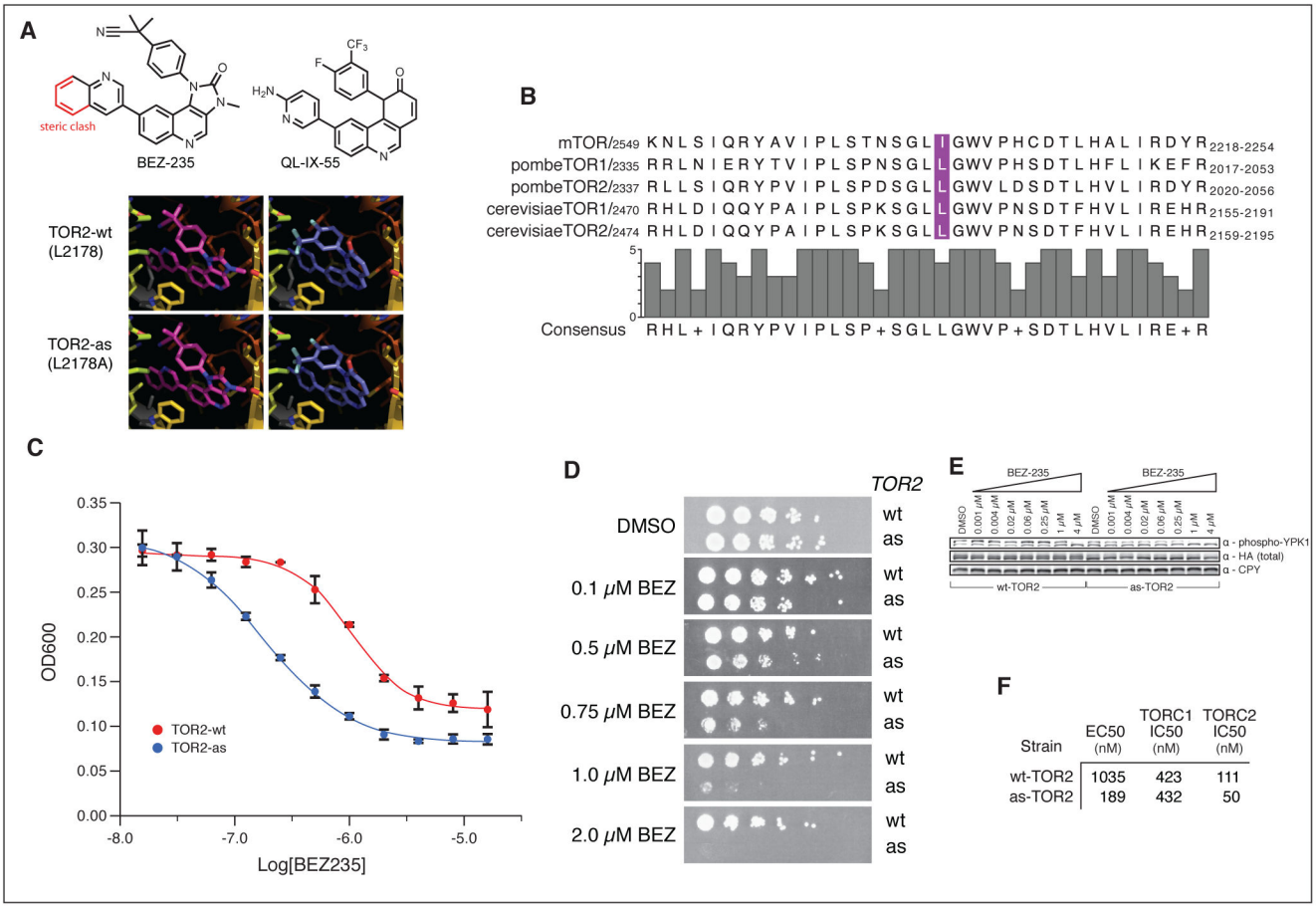

Figure 1. Modeling and Characterization of the as-TOR2 allele

(A) Homology model of mTOR based on the structure of PI3Kγ shown with the gatekeeper residue in gray. The known *S. cerevisiae* TOR1/TOR2 inhibitor QL-IX-55 (purple) and BEZ235 (magenta) are oriented based on a typical h-bonding interaction with the backbone carbonyl of valine in the active site at VanDer Waals distances away from other residues that form the ATP-binding pocket. The isoleucine gatekeeper clash with BEZ235 is exacerbated by mutation to leucine and alleviated by mutation to alanine. The smaller QL-IX-55 does not sense this residue.

(B) Sequence alignment shows the gatekeeper residue (in purple) is isoleucine in mTOR and leucine in all other cases. The active site is highly conserved.

(C) EC50 of as-TOR2 and wt-TOR2 growing in culture. as-TOR2 is significantly more sensitive to BEZ235 than wt-TOR2.

(D) as-TOR2 has an identical growth rate to wt-TOR2 when grown on YPD. At higher doses (1μM BEZ235), growth of as-TOR2 is inhibited while wt-TOR2 is unaffected. Growth of wt-TOR2 begins to be affected at 2μM BEZ235.

(E) *In vivo* phosphorylation of Ypk1 by TORC2 in wt-TOR2 and as-TOR2 containing cells. as-TOR2 is significantly more sensitive to BEZ235 than wt-TOR2.

(F) IC50 values show BEZ235 does not inhibit TORC1, that as-TOR2 does not play a significant role in the catalytic function of TORC1, and that the compound selectively inhibits as-TOR2 in TORC2 over wt-TOR2. The in vitro values correspond well to in vivo results, which are typically less sensitive due to high concentrations of ATP and poor cell wall permeability of yeast.

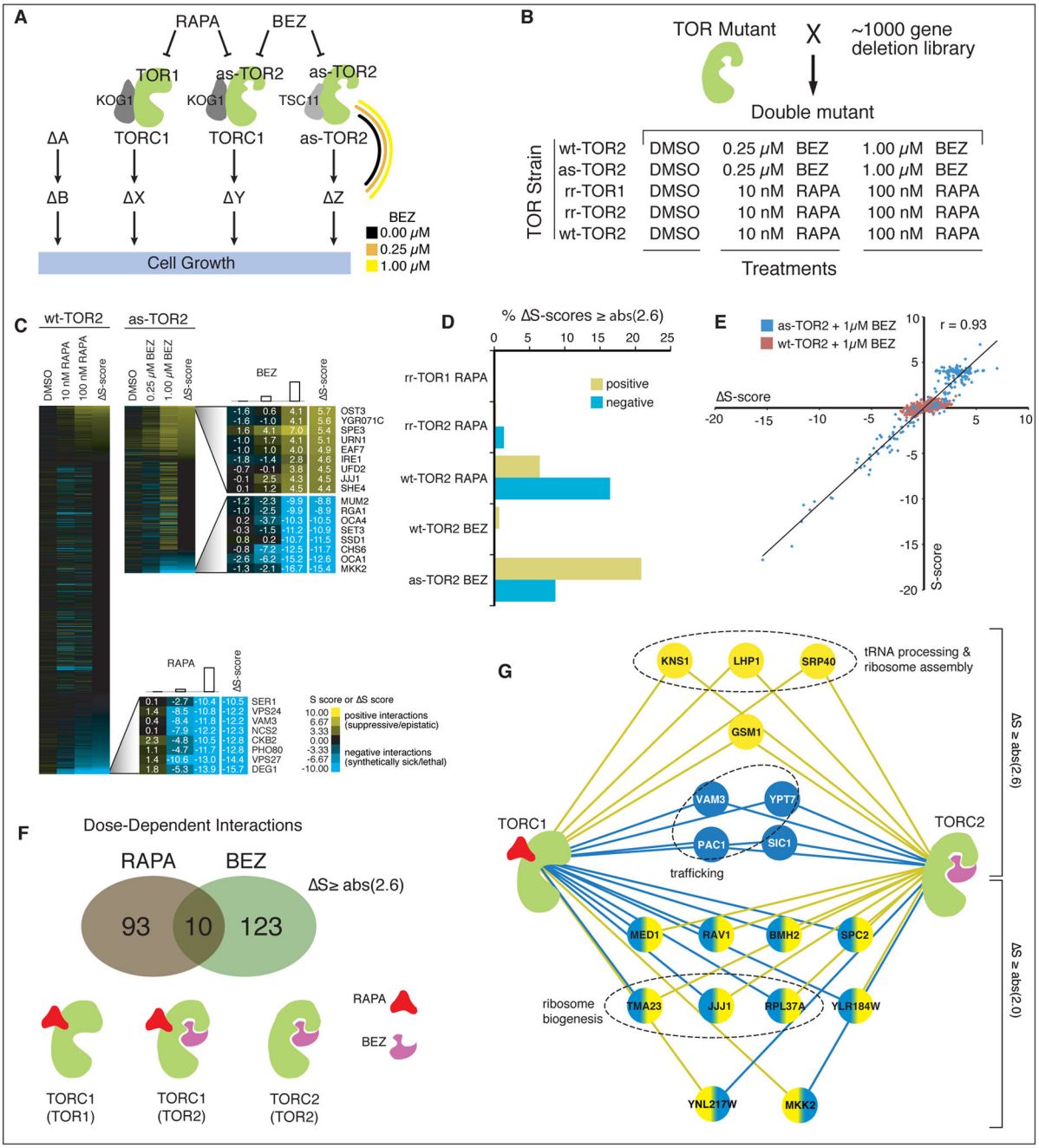

Figure 2. Chemical Epistasis Mapping of TORC1 and TORC2

(A) TOR1 exists only as a member of TORC1. TOR2 may exist as a member of either TORC1 or TORC2. Rapamycin selectively inhibits TORC1. BEZ235 is selective for the as-TOR2 allele. Chemical-genetic interactions behave as traditional double deletion mutants. For interacting genes, a directional shift between the DMSO control and the [high] drug screen should occur. Dose-dependent positive interactions occur between genes in linear pathways, dose-dependent negative interactions occur between genes in parallel pathways.

(B) TOR mutant strains were mated to a library of ~1000 non-essential single deletion mutants. The resulting double mutants were grown on plates containing DMSO or increasing concentrations of rapamycin or BEZ235.

(C) ChE-MAP for rapamycin treated and BEZ235 treated datasets sorted according to ΔS-score. The strength of positive and negative chemical-genetic interactions (S-scores) are reported by yellow or blue squares respectively. Inset are top hits from each set. The as-TOR2 dataset is significantly smaller since many strains were very sick at the highest concentration of BEZ235 and were removed during quality filtering.

(D) Experimental datasets (wt-TOR2+rapa, as-TOR2+BEZ) and control datasets (rr-TOR1+rapa, rr-TOR2+rapa, wt-TOR2+BEZ) are shown by percent of total interactions in the dataset above $\Delta S \geq |2.6|$. Positive interactions are in yellow, negative interactions are blue. Rapamycin and BEZ235 are selective for their intended targets and generate few off target interactions.

(E) Scatterplot of ΔS-score vs S-score illustrates the specific effect of BEZ235 on as-TOR2. wt-TOR2 (red) is unaffected by the compound and cluster around 0. as-TOR2 (blue) is strongly affected and shows a direct relationship between ΔS-score and S-score at 1μM BEZ235.

(F) Number of dose-dependent genetic interactions above a $\Delta S \geq |2.6|$ in each set. 104 interactions recorded for rapamycin, 134 recorded for BEZ with overlap of 10.

(G) Network illustrating genes that hit both TORC1 and as-TOR2 above specified threshold. Nodes and edges are colored yellow for positive or blue for negative interactions with the indicated complex.

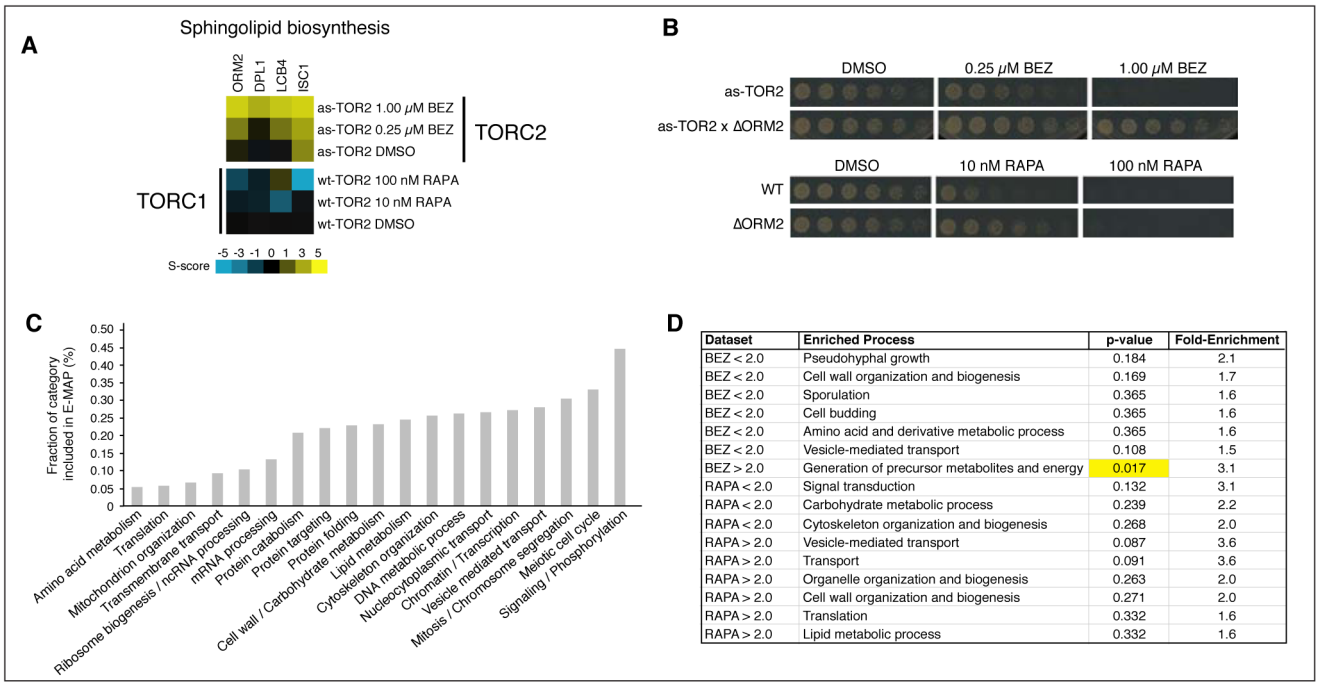

D

Dataset	Enriched Process	p-value	Fold-Enrichment
BEZ < 2.0	Pseudohyphal growth	0.184	2.1
BEZ < 2.0	Cell wall organization and biogenesis	0.169	1.7
BEZ < 2.0	Sporulation	0.365	1.6
BEZ < 2.0	Cell budding	0.365	1.6
BEZ < 2.0	Amino acid and derivative metabolic process	0.365	1.6
BEZ < 2.0	Vesicle-mediated transport	0.108	1.5
BEZ > 2.0	Generation of precursor metabolites and energy	0.017	3.1
RAPA < 2.0	Signal transduction	0.132	3.1
RAPA < 2.0	Carbohydrate metabolic process	0.239	2.2
RAPA < 2.0	Cytoskeleton organization and biogenesis	0.268	2.0
RAPA > 2.0	Vesicle-mediated transport	0.087	3.6
RAPA > 2.0	Transport	0.091	3.6
RAPA > 2.0	Organelle organization and biogenesis	0.263	2.0
RAPA > 2.0	Cell wall organization and biogenesis	0.271	2.0
RAPA > 2.0	Translation	0.332	1.6
RAPA > 2.0	Lipid metabolic process	0.332	1.6

Figure 3. Enrichment in Biological Processes

(A) The sphingolipid biosynthesis pathway shows consistent dose-dependent behavior across all members of the pathway that were included in the screen in good agreement with theoretical prediction. S-score is indicated on a color metric scale with blue as strongly negative and yellow as a strong positive interaction.

(B) Genotyped and sequenced members of pulled tetrads grown on plates containing increasing concentrations of rapamycin or BEZ235 confirm phenotypes tested using the ChE-MAP.

(C) Bar graph shows fraction of each functional biological category that was included in the E-MAP.

(B) Enrichment in either of the two datasets above or below ΔS = 2.0 were calculated using a Fisher's test to identify terms in the cellular process GO Slim that were significantly enriched. Significant p-values highlighted in yellow.

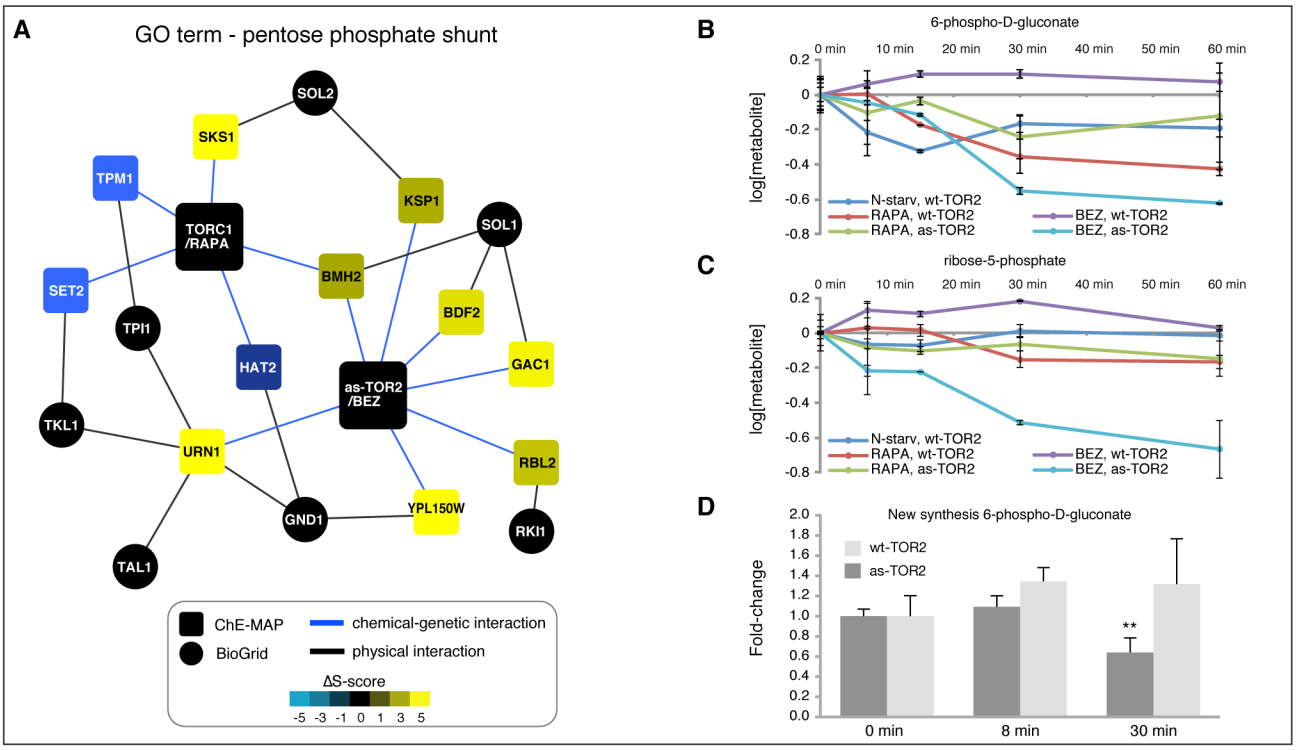

Figure 4. Effect of rapamycin and BEZ235 on metabolites in the PPP

(A) Network of ChE-MAP hits that have physical interactions with genes within the PPP gene ontology term. Rounded rectangles and blue edges indicate chemical-genetic interactions and are colored according to the ΔS-score for the indicated gene. Enrichment for PPP linked genes that positively interact with TORC2 is 2-fold higher than expected by random chance with p = 0.02. Black nodes indicate genes not found in our dataset (www.thebiogrid.org) or in the following citations: (Fan et al., 2008; Fasolo et al., 2011; Graille et al., 2005; Hesselberth et al., 2006; Krogan et al., 2006; Ptacek et al., 2005; Yu et al., 2008). Black edges indicate a physical interaction.

(B) 6-phospho-D-gluconate levels quantified by LC/MS over a 60 minute time-course where cells are perturbed by nitrogen starvation, inhibited with rapamycin (wt-TOR2), or inhibited with BEZ235 or rapamycin (as-TOR2).

(C) Ribose-5-phosphate levels quantified by LC/MS over a 60 minute time-course where cells are perturbed by nitrogen starvation, inhibited with rapamycin (wt-TOR2), or inhibited with BEZ235 or rapamycin (as-TOR2).

(D) Isotope labeled 6-phospho-D-gluconate allows direct measurement of newly synthesized metabolite in as-TOR2 and wt-TOR2 cells and allows quantification of oxidative pentose phosphate pathway flux. Treatment with BEZ235 shows a significant change (**) after the short 30 minute time point.